Characterization of a Plasma Deflagration Accelerator as an ELM Replicator for PFC Testing

K. T. K. Loebner, T. C. Underwood, B. C. Wang, M. A. Cappelli
Department of Mechanical Engineering
Stanford University
Stanford, California 94305
Email: kloebner@stanford.edu

***Abstract*—Transient events in fusion power plants such as DEMO and ITER are known to pose a severe threat to plasma facing components (PFCs) due to melting and erosion after repeated edge localized mode (ELM) loads. Experimental testing *in situ* of potential PFC materials at fusion relevant conditions is difficult and expensive, and no facility currently in operation accurately replicates the salient plasma environment. At Stanford University, an experimental facility designed to mimic the heat flux, particle fluence, and other key characteristics of ELMs and disruption events in a controlled setting is under development. A pulsed plasma accelerator operating in the deflagration mode is used to generate high velocity (40-100 km/s) directed plasma jets that are stagnated on target material samples. In this work, we present probe data characterizing the plasma parameters of the accelerated plume using hydrogen as the working gas, as well as preliminary target studies of copper tokens exposed to pulses at various total and peak shot energies. Results from the probe analysis indicate achieved energy fluxes and heat flux parameters that are ELM-like, and the observed damage morphologies on the witness plates indicate that initial surface roughness plays a significant role in the growth and characteristics of surface melt patterns.**

***Keywords*—plasma jet, plasma-material interface, PMI, first wall, off-normal events, erosion, divertor material**

I. Introduction

As international experimental fusion reactor facilities move closer towards operational status, attention is turning towards the next generation of reactor designs and materials for practical power plants. One of the key engineering challenges in this development is the identification and understanding of the processes occurring at the interface between the plasma exhaust and the reactor first wall, as it is these phenomena that drive the suitability and lifetime of plasma facing components (PFCs) in the reactor, as well as whether the reactor is able to achieve the necessary confinement.

It is known that the bulk of the transient loading experienced by PFCs is the result of edge localized modes (ELMs) and disruption events. As it is difficult to isolate these transient loads in an operating experimental reactor, other techniques have been devised for studying the interaction between plasmas at ELM-like conditions and materials often found in PFCs. These include the use of plasma guns, laser irradiation, and charged particle beams to produce high heat and/or particle fluxes directed onto a target substrate. The latter two techniques can provide heat flux parameters on the order of those expected in ELMs, but may not capture the complex effects that result from a quasi neutral plasma acting as the source of the energy flux. The former technique is the platform that we have chosen to develop at Stanford University, as it is the most flexible and appropriate analog to the conditions experienced in practical fusion machines. By coupling detailed knowledge of the plasma environment both in the jet and the vicinity of the target material, the potential exists for a significantly deeper understanding of the plasma material interactions (PMI) and plasma edge physics that plays a significant and critical role in fusion engineering.

In this work, we experimentally evaluate the Stanford Plasma Gun (SPG) experiment, which is a pulsed plasma accelerator operating in the deflagration regime described extensively in the literature [1]–[5], for use as an analog plasma source designed to replicate ELM-like conditions and behavior. We utilize a Langmuir probe technique to perform low-energy characterization of the plasma jet produced by the Stanford Plasma Gun (SPG) Experiment, described in detail elsewhere [6], [7], using hydrogen as the working gas. In particular, we obtain the energy flux and heat flux parameter of the jet as a benchmark to compare against known ELM behavior [8], in a context similar to that described in Ref. [9]. We then perform a two-parameter target study using copper witness plates, in which we vary the peak and integrated fluxes independently in order to determine which drives the degree and character of the resulting material damage. The witness plate samples are analyzed using a high powered optical microscope with <1 μm resolution. From the combination of these two studies, we show that the observed damage appears to be strongly tied in type and severity to the peak fluxes, and that the morphology of the damage is closely linked to the initial surface characteristics of the target sample.

II. Plume Characterization

In the context of this study, the primary goal of the plume characterization is to obtain a measurement of the bulk heat and particle fluxes experienced by the target surfaces. These measured parameters enable the observed effects on material surfaces to be closely coupled to the plasma conditions, instead of relying on estimates based upon the input energy to the accelerator. To this end, a quadruple Langmuir probe (QLP) was used to obtain the plume parameters necessary to calculate a total energy flux and heat flux parameter to use as a benchmark for comparison against other target studies in the literature.

A QLP is an immersed diagnostic tool that enables simultaneous time-resolved measurements of the plasma density,

978-1-4799-8264-6/15/$31.00 ©2015 IEEE

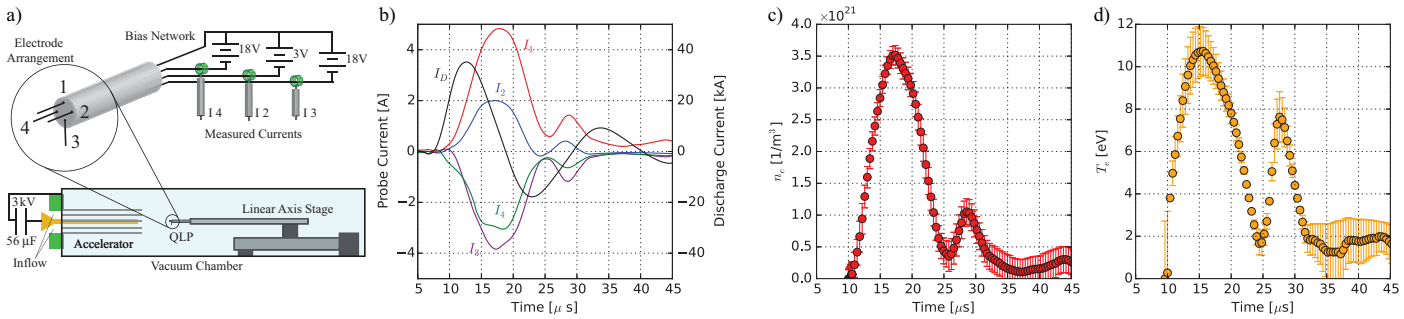

Figure 1: (a) Schematic of the probe construction, bias network, and the probe installed on the linear axis stage in the vacuum chamber along with the Stanford Plasma Gun (SPG). (b) Example current traces collected from the quadruple Langmuir probe (QLP) as well as the corresponding discharge current trace (alternate y-axis). (c) Calculated time-series of the plasma density based on the measured currents. (d) Calculated time-series of the plasma temperature based on the measured currents.

temperature, potential, and ion Mach number at the point location of the probe in the downstream region of the accelerator. The QLP was mounted to a linear axis stage, and by moving the probe along the axis over the course of multiple firings were were able to compile a spatiotemporal contour of each of the plasma state variables. For this study, the probe was operated in current-saturation mode to obtain time-resolved measurements of the resulting plasma plume [10]. The probe as constructed consists of four independent electrodes, as shown in Fig. 1a. Electrodes 1,2, and 4 are oriented parallel to the flow direction while electrode 3 is perpendicular to the flow direction. Electrodes 3 and 4 are nominally biased at -18 V with respect with electrode 1 (ϕ_{13} and ϕ_{14}) while electrode 2 is biased at -3 V (ϕ_{12}).

In order to calculate the four independent plasma state variables, the measured current and associated bias voltages must be coupled with a theory describing the current collected by the probe surface. Similar to other electrostatic plasma probes, the collected probe current, I_p, is composed of contributions due to both electrons and ions and can be written as

$$I_p = I_e - I_i, \tag{1}$$

where I_e and I_i correspond to electron and ion current, respectively. For any electrode exposed to the plasma flow, the collected current will correspond to electron flux if the probe potential is less than the plasma potential ($\phi_{\text{probe}} \leq \phi_{\text{plasma}}$) according to the expression:

$$I_{\parallel e} = A_{\text{probe}} J_{e0} \exp\left[-\frac{e}{kT}\left(\phi_{\text{plasma}} - \phi_{\text{probe}}\right)\right], \tag{2}$$

which is a function of the probe area both parallel and/or perpendicular to the plasma flow direction, A_{probe}, and the thermal diffusion of electrons. Current due to ion collection, however, is a more complex function of the operating regime of the probe. More specifically, the ratio of the local probe radius to the Debye length, r_p/λ_D, and the ratio of ion to electron temperature, T_i/Z_iT_e, governs which theory should be applied. If $5 \leq r_p/\lambda_D \leq 100$ and T_e/Z_iT_i, Ref. 11 developed a relationship for ion current collection as a function of empirical fitting parameters α and β based upon experimental measurements [12],

$$I_{\parallel i} = A_{\text{probe}} J_{i0} \left(\beta + \frac{e}{kT}\left(\phi_{\text{plasma}} - \phi_{\text{probe}}\right)\right)^{\alpha}, \tag{3}$$

$$\alpha = \frac{2.9}{\ln(r_p/\lambda_D) + 2.3} + 0.07\left(\frac{T_i}{Z_iT_e}\right)^{0.75} - 0.34, \tag{4}$$

$$\beta = 1.5 + \frac{T_i}{Z_iT_e}\left[0.85 + 0.135\left(\ln\left[\frac{r_p}{\lambda_D}\right]\right)^3\right]. \tag{5}$$

An analytical expression for the ion current collected by the perpendicular probe in particular was obtained by assuming a negligible sheath thickness [13], i.e. $d_s/r_p \to 1$, such that

$$I_{\perp i} = A_{\perp} n_e e \left(\frac{kT}{2\pi m_e}\right)^{1/2} \frac{2}{\sqrt{\pi}} \exp\left[-S_i^2\right] \sum_{j=0}^{\infty} \frac{S_i^j}{j!}\Gamma\left(j + \frac{3}{2}\right). \tag{6}$$

Coupling these expressions with the assumptions of quasineutrality ($n_e = n$) and thermal equilibrium ($T_i = T_e$) between the electron and ion plasma components, a set of four coupled nonlinear equations for the desired parameters can be developed, giving:

$$I_1 = A_{\parallel} J_{e0} \exp\left(-\frac{e\phi_{p1}}{kT}\right) - A_{\parallel} J_{i0}\left(\beta + \frac{e\phi_{p1}}{kT}\right)^{\alpha}, \tag{7}$$

$$I_2 = A_{\parallel} J_{e0} \exp\left(-\frac{e(\phi_{p1} + \phi_{12})}{kT}\right) - A_{\parallel} J_{i0}\left(\beta + \frac{e(\phi_{p1} + \phi_{12})}{kT}\right)^{\alpha}, \tag{8}$$

$$I_3 = A_{\parallel} J_{e0} \exp\left(-\frac{e(\phi_{p1} + \phi_{13})}{kT}\right) - A_{\parallel} J_{i0}\left(\beta + \frac{e(\phi_{p1} + \phi_{13})}{kT}\right)^{\alpha}, \tag{9}$$

$$I_4 = A_{\perp} J_{e0} \exp\left(-\frac{e(\phi_{p1} + \phi_{14})}{kT}\right) - A_{\perp} n_e e \left(\frac{kT}{2\pi m_e}\right)^{1/2} \frac{2}{\sqrt{\pi}} \exp\left(-S_i^2\right) \sum_{j=0}^{\infty} \frac{S_i^j}{j!}\Gamma\left(j + \frac{3}{2}\right). \tag{10}$$

These equations are solved at each recorded data point in time to obtain a time-series of the derived plasma parameters in a single shot. In the event that $r_p/\lambda_D > 100$, the ion collection theory used in Eqn. 3 is invalid. In this case, a thin sheath is assumed and the ion current follows a Bohm expression [14],

$$I_{\parallel i} = A_{\parallel} n_e e \sqrt{\frac{kT}{m_i}} \exp\left(-\frac{1}{2}\right) \tag{11}$$

Incorporation of this thin sheath assumption lead to the following revised set of current balance equations, valid for a thin sheath $r_p/\lambda_D > 100$:

$$I_1 = A_{\parallel} J_{e0} \exp\left(-\frac{e\phi_{p1}}{kT}\right) - A_{\parallel} n_e e \sqrt{\frac{kT}{m_i}} \exp\left(-\frac{1}{2}\right) \tag{12}$$

$$I_2 = A_{\parallel} J_{e0} \exp\left(-\frac{e(\phi_{p1}+\phi_{12})}{kT}\right) - A_{\parallel} n_e e \sqrt{\frac{kT}{m_i}} \exp\left(-\frac{1}{2}\right) \tag{13}$$

$$I_3 = A_{\parallel} J_{e0} \exp\left(-\frac{e(\phi_{p1}+\phi_{13})}{kT}\right) - A_{\parallel} n_e e \sqrt{\frac{kT}{m_i}} \exp\left(-\frac{1}{2}\right) \tag{14}$$

$$I_4 = A_{\perp} J_{e0} \exp\left(-\frac{e(\phi_{p1}+\phi_{14})}{kT}\right) - A_{\perp} n_e e \left(\frac{kT}{2\pi m_e}\right)^{1/2} \frac{2}{\sqrt{\pi}} \exp\left(-S_i^2\right) \sum_{j=0}^{\infty} \frac{S_i^j}{j!} \Gamma\left(j+\frac{3}{2}\right). \tag{15}$$

The systems described by Eqns. 7-10 and Eqns. 12-15 are solved using a standard Newton-Raphson algorithm with a centered trust region. The initial guess of each state variable provided to the solver are obtained by solving the algebraically-reduced system, which provides a first order solution of the derived plasma parameters. In order to ensure the correct ion collection model is used for each data point, the system of equations corresponding to the thin sheath assumption are solved first, and the resulting Debye length is computed. If r_p/λ_D is such that the theory developed in Ref. [12] is valid, the state variables are recalculated using the equations corresponding to the empirical fit.

A. Results

The probe data was collected at 19 spatial points, ranging from 60-150 mm from the exit plane of the accelerator. The resulting spatiotemporal contours for plasma density and temperature are shown in Figs. 2 and 3, respectively. Using only the density and temperature contours, estimating the bulk plasma velocity via the slope of the leading edge of the plasma density contour, we calculate the relevant bulk energy flux and heat flux parameter for the jet. This data was collected only for the 3 kV charging voltage, corresponding to 252 J, due to the fact that at higher energies it was not technically feasible to collect probe data this close to the exit plane of the accelerator as a result of arcing.

The energy flux ($\mathscr{E}$) is assumed to consist entirely of internal (thermal) energy of the flowing plasma and the kinetic

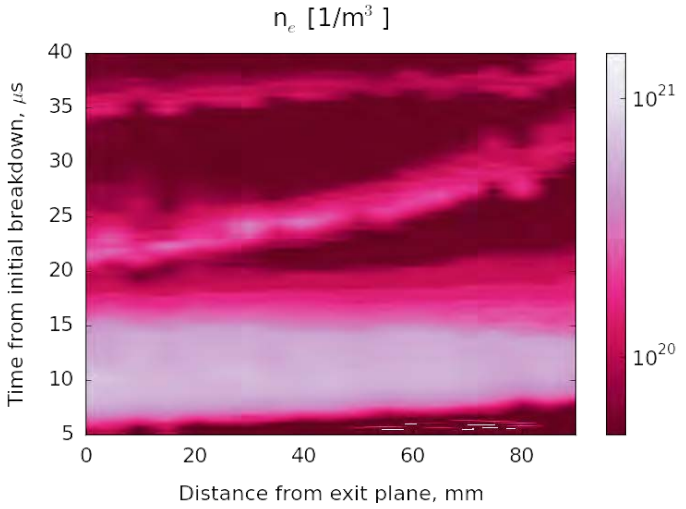

Figure 2: Contour of the plasma density along the axis as a function of time. Three plasma ejections are clearly visible, corresponding to three ringdown oscillations of the driving capacitor bank. Peak densities are of 10^{21} m^{-3} are observed in the initial deflagration jet.

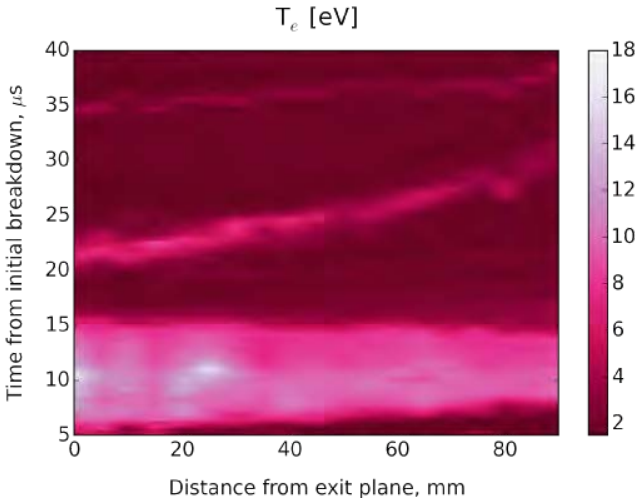

Figure 3: Contour of the plasma / electron temperature along the axis as a function of time. Structure of the temperature contour is less pronounced, particularly for the second and third ejections. An overall mean temperature of ∼10-12 eV is observed in the initial deflagration jet, and the effective pulse width experienced by the target is determined based on this contour to be ∼10 μs.

energy carried by the plasma jet. This is calculated as

$$\mathscr{E} = \tilde{c}_v T_e \cdot n_e V + \frac{1}{2} m_p V^2 \cdot n_e V$$

where $\tilde{c}_v$ is the per-particle heat capacity of hydrogen at constant volume (assumed to be $\frac{3}{2}k_B$), T_e is the plasma temperature (where we have assumed that $T_e = T_i$ as per the QLP theory), m_p is the proton mass, n_e is the plasma density and V is the bulk jet velocity. Using the nominal values from the probe data of $T_e \simeq 10$ eV, $n_e \simeq 10^{21}$ m^{-3}, and

$V \simeq 40$ km/s (obtained via the slope of the leading edge of the spatiotemporal contour), we obtain an energy flux of

$$\mathscr{E} \simeq 150 \text{ MW m}^{-2}$$

For a nominal pulse with of $\sim$10 μs (obtained from the width of the plasma pulse in the contours), the heat flux parameter ($\mathscr{H}$) is thus

$$\mathscr{H} = 0.58 \text{ MW m}^{-2} \text{ s}^{-1/2}.$$

This is somewhat lower than the heat flux parameter typically used to replicate ELMs in systems developed by others [15]. However, this apparent shortcoming is mitigated for two reasons: first, this heat flux parameter is based on measured data in the plasma plume, so it is not immediately apparent that this is in fact a significantly lower number than that actually realized by systems based on optical heating, given the lack of actual heat flux data in those cases. Second, we expect the heat flux parameter to scale approximately linearly with input energy, and this data was collected at a comparatively low input energy ($\sim$250 J/pulse). The heat flux parameter is therefore likely to be in the range of 4.1 MW m^{-2} s$^{-1/2}$ at the highest pulse energy tested in this study. Furthermore, the overall energy flux is higher than that generally associated with ELMs.

III. Witness Plate Target Study

In an effort to determine the type and degree of damage caused by the accelerated plasma jets, a series of experiments using witness plates was performed as a means of investigating the bulk effects of the jet on the sample. The targets used were unpolished, 'mirror-finish' pure copper tokens, placed normal to the flow direction along the central axis of the accelerator. The target was located $\sim$10 cm from the exit plane of the accelerator, and held in a sample holder mounted to the linear axis stage; the stage was kept at the same position for all trials.

The objective of this study was twofold: first, to establish a baseline characterization of whether the facility can produce observable damage on a target substrate, and second, to preliminarily investigate what input parameters of the facility drive the scale and qualitative aspects of the observed damage.

A. Results

The optical micrographs of the series of targets irradiated by the SPG facility are shown in Fig. 4. Since the copper targets were not additionally polished beyond the stock 'mirror finish' prior to exposure, the initial surface characteristics displayed a fairly large degree of initial roughness on the micro scale (shown in Fig. 4a) due to residual machining marks. However, this led to what is one of the more interesting results of the target study: the damage from the impinging plasma jet was observed to localize preferentially along the linear grooves in the material. Examples of this are clearly visible in Figs. 4f, 4g, and 4l. The latter micrograph shows the boundary between the exposed and unexposed portions of the witness plate, where the transition from unexposed linear grooves to linearly-structured damage zones is clearly visible.

The additional objective of the target study was to determine whether total energy flux, i.e. over multiple low-energy shots, would achieve the same types of damage generated by a single high-energy-flux shot. As is clearly visible from the micrographs, equivalent total energy fluxes do not produce the same results. For example, the SPG fired ten times at 2.0 kV (Fig. 4j) corresponds to the same total energy flux as the SPG fired at 6.32 kV a single time (Fig 4f). This comparison assumes that the actual energy flux in the jet correlates to the initially stored energy in the capacitor bank, but it is evident that even if there is a moderately non-linear scaling of the jet parameters with energy, that the damage sustained is much more strongly dependent on the peak fluxes experienced by the target.

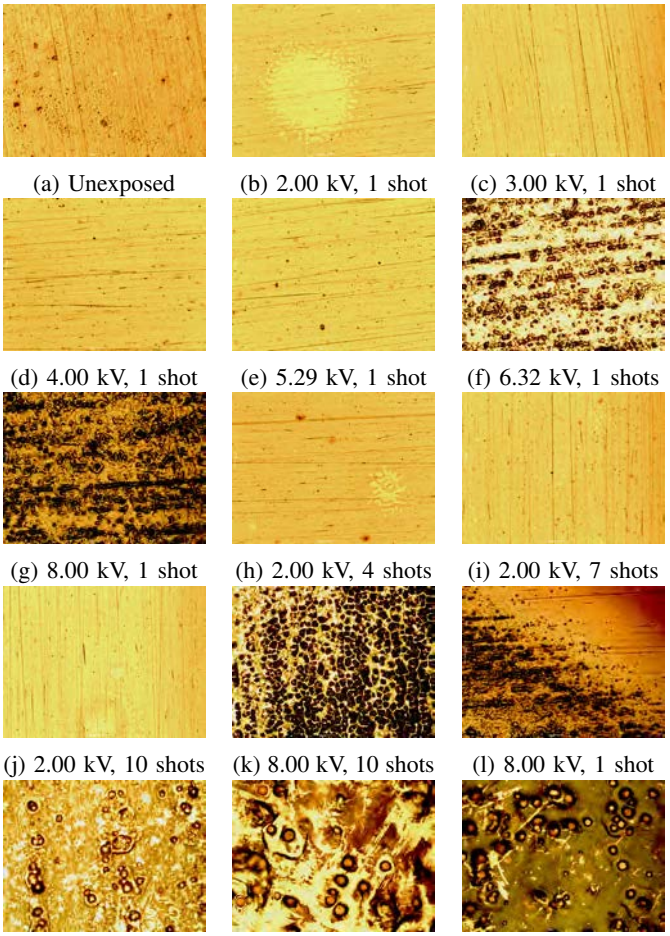

Figure 4: Compilation of optical micrographs corresponding to all the tested conditions in the witness plate study. Subfigures (a)-(l) correspond to the same magnfication (scale bar visible), whereas subfigures (m)-(o) are images taken at a higher magnification.

In the higher magnification micrographs (Figs. 4m-o), we can clearly see signs that the copper target melted during exposure and subsequently re-solidified. This indicates that the target was heated to at least 1358 degrees Kelvin, the melting point of pure copper. This is a strong indication that the Stanford Plasma Gun is generating the conditions necessary to properly replicate the effects of ELMs in fusion-scale tokamak devices.

IV. Conclusion

We have presented work that provides preliminary indications that the SPG facility is suitable for generating ELM-like loads for testing candidate PFC materials and configurations. Though the overall fluence and energy density remains somewhat below that expected for single ELM events in the regimes tested, the peak fluxes are sufficiently large at high energy (> 1 kJ/pulse) that the shortcoming in net energy and heat flux can be mitigated over the course of multiple firings. Furthermore, the facility is capable of operating at maximum energies of 12 kJ/pulse, i.e. one order of magnitude higher input energy , and thus the predicted energy densities for ELM events are at least theoretically attainable over the course of a single shot.

The data collected via the QLP enabled the calculation of the direct plasma parameters necessary to determine the bulk energy flux of the jet, and the target studies indicated that achieving the requisite damage threshold is a strong function of the peak energy flux. The target studies also provided a promising avenue for further work, studying the specific mechanism responsible for damage localization at initial sites of surface irregularity. One explanation is the reduced ability of the substrate to conduct heat away from the increased surface area in the vicinity of the groove, as well as increased field electron emission from the surface in the vicinity of the sharp groove edges driving higher ion fluxes into the surface. In any event, this interesting result shows why the proper evaluation of potential PFCs under fusion conditions requires the use of high energy plasma sources such as the SPG facility, in order to capture the complex interaction of the plasma and material interface.

Acknowledgment

This work is sponsored by the U.S. Department of Energy (DoE) Stewardship Science Academic Program (SSAP), Grant No. DE-NA0002011. Authors K. Loebner, B. Wang, and T. Underwood gratefully acknowledge the support of the National Defense Science and Engineering Graduate (NDSEG) Fellowship, 32 CFR 168a.

References

[1] D. Y. Cheng, "Plasma deflagration and the properties of a coaxial plasma deflagration gun," *Nuclear Fusion*, vol. 10, no. 3, pp. 305–317, Sep. 1970. [Online]. Available: http://stacks.iop.org/0029-5515/10/i=3/a=011?key=crossref.653d85b404f52df711f900156dbf3e56

[2] D. M. Woodall and L. K. Len, "Observation of current sheath transition from snowplow to deflagration," *Journal of Applied Physics*, vol. 57, no. 3, p. 961, 1985. [Online]. Available: http://scitation.aip.org/content/aip/journal/jap/57/3/10.1063/1.334697

[3] R. Wallace, "Theoretical, computational and experimental analysis of the deflagration plasma accelerator and plasma beam characteristics," Ph.D. dissertation, Virginia Polytechnic Institute and State University, 1991. [Online]. Available: http://adsabs.harvard.edu/abs/1991PhDT.....197W

[4] J. T. Bradley, "Diagnostics and analysis of incident and vapor shield plasmas in PLADIS I, a coaxial deflagration gun for tokamak disruption simulation," *IEEE Transactions on Plasma Science*, vol. 27, no. 4, pp. 1105–1114, 1999.

[5] Y. Thio, R. Eskridge, and M. Lee, "An Experimental Study of a Pulsed Electromagnetic Plasma Accelerator," in *38 th AIAA/ASME/SAE/ASEE Joint Propulsion Conference and Exhibit*, Indianapolis, IN, 2002. [Online]. Available: http://arc.aiaa.org/doi/pdf/10.2514/6.2002-4269

[6] F. Poehlmann, "Investigation of a Plasma Deflagration Gun and Magnetohydrodynamic Rankine-Hugoniot Model to Support a Unifying Theory for Electromagnetic Plasma Guns," Ph.D. dissertation, Stanford University, 2010.

[7] K. T. K. Loebner, B. C. Wang, F. R. Poehlmann, Y. Watanabe, and M. A. Cappelli, "High-Velocity Neutral Plasma Jet Formed by Dense Plasma Deflagration," *IEEE Transactions on Plasma Science*, vol. 42, no. 10, pp. 2500–2501, Oct. 2014. [Online]. Available: http://ieeexplore.ieee.org/lpdocs/epic03/wrapper.htm?arnumber=6849459

[8] A. W. Leonard, "Edge-localized-modes in tokamaksa)," *Physics of Plasmas*, vol. 21, no. 9, p. 090501, Sep. 2014. [Online]. Available: http://scitation.aip.org/content/aip/journal/pop/21/9/10.1063/1.4894742

[9] S. Jung, V. Surla, T. K. Gray, D. Andruczyk, and D. N. Ruzic, "Characterization of a theta-pinch plasma using triple probe diagnostic," in *Journal of Nuclear Materials*, vol. 415, no. 1 SUPPL, 2011.

[10] N. A. Gatsonis, J. Zwahlen, A. Wheelock, E. J. Pencil, and H. Kamhawi, "Characterization of a pulsed plasma thruster plume using a quadruple langmuir probe method," *AIAA Paper*, vol. 4123, p. 2002, 2002.

[11] E. Peterson and L. Talbot, "Collisionless electrostatic single-probe and double-probe measurements," *AIAA Journal*, vol. 8, no. 12, pp. 2215–2219, 1970.

[12] J. Laframboise, "Theory of cylindrical and spherical langmuir probes in a collisionless plasma at rest," in *Rarefied Gas Dynamics, Volume 2*, vol. 1, 1965, p. 22.

[13] B. H. Johnson and D. Murphree, "Plasma velocity determination by electrostatic probes," *AIAA Journal*, vol. 7, no. 10, pp. 2028–2030, 1969.

[14] S.-L. Chen and T. Sekiguchi, "Instantaneous direct-display system of plasma parameters by means of triple probe," *Journal of Applied Physics*, vol. 36, no. 8, pp. 2363–2375, 1965.

[15] I. E. Garkusha, N. I. Arkhipov, N. S. Klimov, V. A. Makhlaj, V. M. Safronov, I. Landman, and V. I. Tereshin, "The latest results from ELM-simulation experiments in plasma accelerators," *Physica Scripta*, vol. T138, p. 014054, 2009.